Journal of Non-Crystalline Solids 358 (2012) 1687–1698

Contents lists available at SciVerse ScienceDirect

Journal of Non-Crystalline Solids

journal homepage: www.elsevier.com/ locate/ jnoncrysol

Enthalpy relaxation of comb-like polymer analysed by combining activation energy spectrum and TNM models

Y. Tanaka *, T. Yamamoto

Department of Material Science and Engineering, Faculty of Engineering, University of Fukui, Fukui 910-8507, Japan

ARTICLE INFO

Article history:
Received 14 December 2011
Received in revised form 28 April 2012
Available online 25 May 2012

Keywords:
Structural relaxation;
Comb-like polymer;
Glass transition;
Activation energy;
TNM model

ABSTRACT

In the enthalpy relaxation of poly(cyanobiphenyl ethylacrylate) (PCB2A), the decrease in enthalpy was measured as a function of ageing time and ageing temperature with DSC technique. Obtained data was analysed at first with the activation energy spectrum (AES) model, then compared with the prediction of a multi-parameter phenomenological model which follows the evolution of the configurational entropy (SC) of the sample during the whole thermal history. In AES model, the decrease in enthalpy is controlled by molecular processes whose energies are distributed over a continuous spectrum. The spectrum gives the relation between the number and energy of processes. In consequence, AES of a single peak was obtained. The energy at which the peak maximum was located decreased with the increase in ageing temperature, which is a well-known behaviour as a distribution of relaxation processes. Furthermore, $c_p(T)$, the heat capacity data obtained by the calculation based on SC model reproduced the experimental $c_p(T)$ curve. Model parameters found in the calculation was discussed in relation to the energy value of AES maximum.

1. Introduction

The effect of physical ageing on glassy polymer has been studied extensively via several experimental methods. Of interest in these experimental methods is the continuous evolution of the thermodynamic state towards equilibrium [1,2]. The evolution of the thermodynamic state is referred to as structural relaxation, and is accompanied by changes in various properties. Many studies have reported on these various properties, including volume recovery [3,4], viscosity [5], creep compliance [6–8], stress recovery [9]. The interrelationships between these properties are considered using the linear viscoelastic functions. This is making further progress towards the modelling technologies [10–12].

Among the different experimental methods, the differential scanning calorimetry (DSC) is frequently used to investigate the enthalpy relaxation. Analytical methods for the result of DSC are also being developed on the basis of the thermodynamic state variables. The variables employed are the configurational entropy, S_c and the fictive temperature, T_f [13,14]. Most of the analytical methods are based on the framework of Tool–Narayanaswamy–Moynihan (TNM) approach [14–16]. In the TNM approach the relaxation functions of infinitesimal intervals and Boltzmann superposition principle are combined. This approach has both positive and negative attributes. On the one hand, the TNM framework succeeds in reproducing the curve of the heat capacity, $c_p(T)$ for many materials, on the other hand, several issues are raised for the processes of $c_p(T)$ calculation.

Some of the unresolved issues found in literatures are described here; the mathematical model is comprised of model parameters which have strong dependence of thermal history [17–19]. The TNM framework was firstly tested on the experimental data of inorganic glasses, and the implicit assumption for polymers to be treated like inorganic glasses could be questionable; in particular, the characteristics of polymer cannot be found in the models at all, for example, molecular weight, gyration radius, chain architecture and so on [17,20,21]. The effect of thermal lag inside the DSC cup cannot explain the discrepancies between model calculation and experimental results [22–24].

The TNM framework, despite its incompleteness, is still the model of choice for approaching the glass transition and structural recovery due to its ability to capture all of the phenomenology associated with the glass transition kinetics.

In this work, we attempted to improve TNM framework by accounting for the parameter of the energy constant used in the model of the configurational entropy (SC model). Concerning $c_p(T)$ calculations of the model of both T_f and S_c, the expressions for the relaxation time are shown below.

$$\tau = A\exp\left(\frac{x\Delta h}{RT} + \frac{(1-x)\Delta h}{RT_f}\right) \quad (1)$$

$$\tau = A\exp\left(\frac{B}{TS_c}\right) \quad (2)$$

* Corresponding author. Tel.: +81 776 27 8974; fax: +81 776 27 8767.
E-mail address: tanaka@matse.u-fukui.ac.jp (Y. Tanaka).

0022-3093/$ – see front matter © 2012 Elsevier B.V. All rights reserved.
doi:10.1016/j.jnoncrysol.2012.05.003

Eq. (1) is a generalised version of the Arrhenius type, whereas Eq. (2) is proposed using the molar Gibbs free energy barrier of B for the equilibrium relaxation time of glass-forming liquids taking into account of the transition probability of a cooperative region. Although both expressions often can be seen in the TNM framework, the model of T_f is more frequently seen than SC model, particularly over the last few years. Nevertheless, the reasoning of SC model is not at a disadvantage compared to the model of T_f, rather, some shortcomings of Eq. (1) are suggested in capturing the structure dependence of relaxation time [17,23,25].

The investigation whether each of these τ-expressions fits or not to the results of our experiment is outside of this work. This work is to contribute to the determination of the material parameters such as A, B, etc. As a background, it must be remarked that the independent determination for B value has not yet been accomplished. To overcome an indeterminate B value, the activation energy spectrum (AES) was introduced as a proposal to be related to the model parameter.

AES model provides information about thermally activated processes which are available to contribute to observed changes in the polymer properties as it ages. By "processes", we are referring to any thermally activated rearrangement of single atoms or atom groups. In glassy polymers, it can be considered that the rearrangement is caused by the motion in a segmental unit. In relation to the rearrangement, extensive theoretical and experimental works have been carried out on local dynamics of polymers in bulk to elucidate the mechanism of conformational transitions [27]. As a result, some reasonable mechanisms of the conformational transitions are proposed, these include a crankshaft-like motion such as the Schatzki crankshaft [28], three-bond motions [29], simultaneous rotation about three parallel bonds [30]. However, it is difficult to tell clearly at present the mode of dynamics in segmental unit during the thermal ageing right after the cooling from the high temperature. The participant in the motion of the segmental unit is also ambiguous particularly for the comb-like polymer as used in this work. Therefore, the term of the local dynamics as used in this paper means the segmental motion which brings about the processes of rearrangement, and eventually causes the decrease in enthalpy. Consequently, the analysis of AES model gives the distribution of the relaxation process.

With these backgrounds, this paper is concerned with the $c_p(T)$ curve obtained by DSC measurement for comb-like polymer having cyanobiphenyl group. The sample is poly(cyanobiphenyl-yloxy) ethyl acrylate (abbreviated as PCB2A). The reason of examining the comb-like polymer is the significant variation of free volume in glass transition, which is expected to lead to the observable enthalpy decrease upon experimental ageing time. Research reports on enthalpy relaxation are seen for samples of liquid crystalline polymer of side chain type, presumably with similar ideas [31–34].

2. Theoretical framework

2.1. Calculation of activation energy spectrum

The activation energy spectrum was calculated following the method of Gibbs et al. [35]. The spectrum provides the distribution of the energy and the molecular process, and accounts for properties of PCB2A. The decrease in enthalpy that occurs in PCB2A upon isothermal ageing below T_g can be represented as,

$$\Delta H(t_A, T_A) = \Delta H(\infty, T_A) \times (1 - \phi). \tag{3}$$

$\Delta H(t_A, T_A)$ is the decrease in enthalpy for the experimental ageing time and temperature of t_A and T_A. $\Delta H(\infty, T_A)$ is the limiting value of $\Delta H(t_A, T_A)$ as $t_A \to \infty$, ϕ is the relaxation function expressed as,

$$\phi = \exp\left[-(t_A/\tau)^{\beta}\right] \tag{4}$$

The relaxation time, τ, and the shape parameter, β, where $0 < \beta \leq 1$, characterise this function, and are considered to be constant for constant t_A [18]. Furthermore, the enthalpy change has been shown in the relaxation model of Narayanaswamy in integral form with a certain response function, $R(\xi)$ [7,14].

$$\delta_H(\xi) = \Delta c_p \int_0^{\xi} R(\xi - \xi') \frac{dT}{d\xi} d\xi' \tag{5}$$

Δc_p is the heat capacity increment at the glass transition; the time variable is the reduced time ξ which expression is described in the next section. $\delta_H(t_A)$ is equivalent with the departure from the equilibrium at T_A and can be taken as the measure of structure where,

$$\delta_H(t_A) = \Delta H(\infty, T_A) - \Delta H(t_A, T_A) \tag{6}$$

$\delta_H(t_A)$ is controlled by molecular processes whose activation energies, E, are distributed over a continuous spectrum according to the AES model. This model predicts that $\Delta H(t_A, T_A)$ can be obtained by the integral,

$$\Delta H(t_A, T_A) = \int_0^{kT_A \ln(\nu_0 t_A)} P(E) dE \tag{7}$$

$P(E)$ is the enthalpy change related to the process with activation energies in the range between E and $E + dE$, and is expressed by

$$P(E) = c(E) \times q_t(E) \tag{8}$$

$q_t(E)$ is the number density of processes of activation energy E. The processes contribute to the change in enthalpy with the elapsed time of t_A. $c(E)$ is the measured enthalpy change if only one process having activation energy of E is thermally activated per unit volume of material. In practice, more than one type of single atom or multi-atom process may have the same value of activation energy, that is, $c(E)$ will then depend on the type of process occurring with the energy value E. The processes can be regarded, without loss of generality, as being all of one type with a single average value of $c(E)$. ν_0 is the frequency factor for single atom process. The value of ν_0 is on the order of 10^{-12}/sec which is derived from the frequency of the Debye temperature [35]. From Eqs. (3) and (7), the expression to derive the relation of $P(E)$ and E can be given.

$$P(E) = -\frac{\Delta H(\infty, T_A)}{kT_A} \cdot \frac{d\phi}{d \ln t_A}\Big|_{t_A = \frac{1}{\nu_0} \exp \frac{E}{kT_A}} \tag{9}$$

In AES, E was expressed as the energy per mole. In addition, $P(E)$ was expressed nominally as the number of processes in this work. Therefore, Eq. (9) implies that the total of all energies will be equivalent with $\Delta H(\infty, T_A)$, if they are added up in the range $0 < E < \infty$ at the constant temperature of T_A. As mentioned above, because the participant of local dynamics is ambiguous, the unit of $P(E)$ is somewhat unclear. To conclude, $P(E)$ is shown as the relative value of the number of processes in the following section. The spectrum gives information about the processes controlling the relaxation. A similar treatment to derive AES can be found for the enthalpy relaxation of inorganic glasses and liquid crystalline polymer [34,36].

2.2. Calculation of $c_p(T)$ curve by TNM framework with SC model

The TNM formalism attempts to describe the glass transition as a kinetic phenomenon, and takes the two main features for structural relaxation, those are non-exponential and non-linear character [31,37]. To account for the former character, in general, the relaxation is expressed using a stretched exponential function of Eq. (4).

Non-linear effects can be expressed that the instantaneous relaxation rate depends on both the temperature and the glassy structure

developed in the sample during the ageing process; the parameter to measure the structural state is the configurational entropy, that is, $\tau = \tau[S_c(t), T(t)]$. S_c at a time t is regarded as a function of the entire temperature history the sample had gone through up to t and $T(t)$. The equation of τ is assumed to have the same form as Adam and Gibbs' formula of Eq. (2), which was originally intended by the authors only for equilibrium [38,39]. In fact, if the configurational entropy in Eq. (2) has the equilibrium value $S_c^{eq}(T)$, it gives the equation of:

$$\tau^{eq}(T) = A\exp\left(\frac{B}{S_c{}^{eq}(T)\cdot T}\right) \tag{10}$$

which defines Adam and Gibbs' curve of the equilibrium relaxation time, $\tau^{eq}(T)$. The parameter A is the pre-exponential factor. B is related to the microscopic picture of the process through $B = s_c\,\Delta\mu/k$, where $\Delta\mu$ is the free energy barrier hindering configurational rearrangement per mol of molecules or chain segments. s_c is the configurational entropy of the smallest cooperatively rearranging region, which is analogous to $c(E)$ of the enthalpy change in AES model.

The evolution of the configurational entropy in response to a thermal history that consists of a series of temperature jumps from T_{i-1} to T_i at time instants t_i followed by isothermal stages, is given by

$$S_c(\xi, T) - S_c^{eq}(T) = \sum_{i=1}^{n}\left(\int_{T_{i-1}}^{T_i}\frac{\Delta c_p}{T}\,dT\right)\phi(\xi-\xi_i). \tag{11}$$

By rescaling the experimental time to the reduced time of ξ, S_c can be expressed as a function of t,

$$\xi = \int_0^t \frac{d\lambda}{\tau(\lambda)} \tag{12}$$

where $\xi_i = \xi(t_i)$. Further, it is assumed that if the sample is subjected to an arbitrary temperature program, the state attained by the material as the progress of time without limit is uniquely determined by T, and is independent of further details of temperature history. For this *limit state*, a function $S_c^{lim}(T)$ exists, which depends only on temperature, and gives the limit value of $S_c(t)$ in such a process as just described when $t \to \infty$. If the limit state of the structural relaxation process coincides with the extrapolation of the equilibrium values determined at temperatures above T_g, $S_c^{lim}(T) = S_c^{eq}(T)$ could be given with,

$$S_c^{eq}(T) = \int_{T_2}^{T}\frac{\Delta c_p(\theta)}{\theta}\,d\theta. \tag{13}$$

where $\Delta c_p(T) = c_{pl}(T) - c_{pg}(T)$ is the configurational heat capacity, the difference in the heat capacity between equilibrium liquid and glass at the same T. T_2 is the equilibrium second order-transition temperature.

It should be noted for the relaxation function of ϕ appeared in Eq. (11). Strictly speaking, ϕ of Eq. (11) is not the same as that of Eq. (3); while ϕ of Eq. (11) expresses the relaxation after the temperature jump from T_{i-1} to T_i and has the form of reduced time domain, Eq. (3) is the relaxation function during the ageing and in the form of real time domain. However, ϕ of Eq. (3) seems to be expressed with the data of reduced time domain, because the decrease in enthalpy is also expressed with the integral of reduced time (see Eqs. (3) and (5)). The same ϕ function, and therefore the same value of β, was applied for both Eqs. (3) and (11).

It is supposed here that, after rescaling time, the non-linear function can be expressed in the form of a 'quasilinear' relationship between $S_c(t)$ and $T(\xi)$.

$$S_c(t) = S_c{}^{lim}(T) - \sum_{i=1}^{n}\left[S_c^{lim}(T_i) - S_c^{lim}(T_{i-1})\right]\times\phi[\xi(t)-\xi(t_{i-1})] \tag{14}$$

Further, the limiting value of $\Delta c_p(T)$ can be written as $\Delta c_p^{lim}(T) = c_p^{lim}(T) - c_{pg}(T)$ and,

$$\Delta c_p^{lim}(T) = T\frac{dS_c^{lim}(T)}{dT} \tag{15}$$

$S_c^{lim}(T)$ is calculated as

$$S_c^{lim}(T) = S_c^{eq}(T^*) + \int_{T^*}^{T}\frac{\Delta c_p^{lim}(\theta)}{\theta}\,d\theta \tag{16}$$

In Eq. (16), T^* is a temperature above T_g in the equilibrium liquid state, where the limit state coincides with the equilibrium state. $T^* = T_g + 10$ °C was taken in this study.

By applying the set of these equations to the thermal history, the expression of $S_c(t)$ is derived.

$$S_c(t) = S_c^{lim}[T(t)] - \sum_{i=1}^{n}\left(\int_{T_{i-1}}^{T_i}\frac{\Delta c_p^{lim}(\theta)}{\theta}\,d\theta\right)\times\exp\left[-\left(\int_{t_{i-1}}^{t}\frac{d\lambda}{\tau(\lambda)}\right)^{\beta}\right] \tag{17}$$

The resulting equation has four adjustable parameters: A, B, T_2 and β. Three of them, A, B, T_2, together with $\Delta c_p^{lim}(T)$ define the dependence of the equilibrium relaxation times from Eq. (10).

Eqs. (13–17) must be solved numerically. In this work the cooling and heating in the thermal histories were replaced by a series of 0.5-degree temperature jumps followed by isothermal stages with a duration calculated to result in the same overall rate of temperature change as in the actual experiments. For the specified temperature the configurational entropy was calculated with Eq. (17), then the relaxation time corresponding to that configurational entropy was calculated using Eq. (2).

The analysis requires to express the experimental results and calculated values in terms of $\Delta c_p(T)$ curves, whereas there is no straightforward relationship between the configurational entropy and $c_p(T)$. However, the following relation can be used;

$$c_p(T) - c_{pg}(T) = dH_c/dT \tag{18}$$

where H_c is the specific configurational enthalpy. For the dependence of H_c on the thermal history, the same manipulation as used for $S_c(t)$ is applied.

$$H_c(t) = H_c^{lim}[T(t)] - \sum_{i=1}^{n}\left(\int_{T_{i-1}}^{T_i}\Delta c_p^{lim}(T)\,dT\right)\times\exp\left[-\left(\int_{t_{i-1}}^{t}\frac{d\lambda}{\tau(\lambda)}\right)^{\beta}\right] \tag{19}$$

The assumption made here in order to determine H_c(t) is that enthalpy and entropy have the same relaxation function ϕ; in other words, the relaxation times for enthalpy and entropy are same. $c_p(T)$ evaluated using Eq. (18) was compared with the experimental result.

It is necessary to make an additional assumption on $c_p^{lim}(T)$ because we have no information concerning the temperature dependence of $c_p^{lim}(T)$. Its phenomenological shift of δ in the heat capacity with respect to $c_{pl}(T)$ was taken into consideration as depicted in Fig. 1 in a narrow temperature range around T_g to account for the overestimation of the enthalpy of polymer appeared in TNM. The phenomenological shift of δ-parameter has been widely accepted in applying SC model [37,40–42]. As for the evaluation of c_p, the temperature dependence of S_c is shown in Fig. 1 for the liquid state (equilibrium), for an experimental scan at finite rate (solid line), and for the hypothetical limit of the structural relaxation process. This metastable limit, intermediate between liquid and glass, is distinctive of polymers and could originate from a collapse of the configurational rearrangements of polymer chains when the rearrangements reach a limit, for example, by the presence of topological constraints.

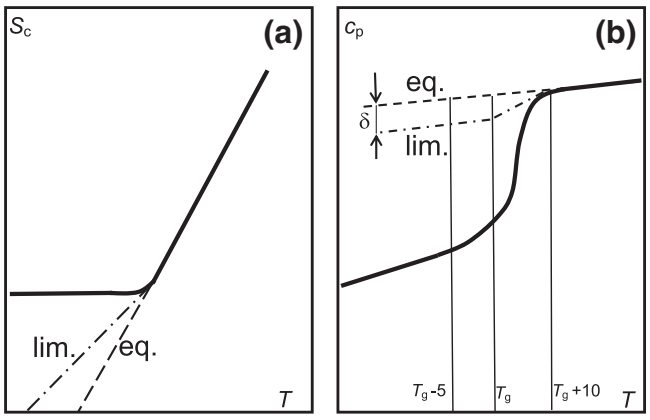

Fig. 1. (a) Schematic representation of the configurational entropy, S_c, corresponding to the liquid state denoted by 'eq.' (dashed line), to the experimental scan at a finite cooling rate (solid line), and to the metastable state denoted by 'lim', hypothetical limit of the structural relaxation process (dashed-dotted line). (b) $c_p(T)$ lines corresponding to three cases shown in (a): the dashed line corresponds to the liquid state, the solid line corresponds to the experimental cooling scan, and the dashed-dotted line corresponds to $c_p(T)$ in the limit states of the structural relaxation process.

We have employed simultaneous fitting procedures, with the aim of reproducing six different DSC curves obtained for the thermal history of the constant ageing temperature. (The number of DSC curves varied depending on the set of measurements.) For equations shown above, the unknowns are A, B, T_2, β and δ. An iterative search routine was used to determine the best single set of these parameters with reference to the method of function minimisation [43,44]. That is, the successive substitutions of the parameters were carried out to find the minimum of the average square deviation defined as

$$\sigma_a = \frac{1}{6N}\sum_{i=1}^{6}\sum_{j=1}^{N}\left[w(i)\left\{c_{p,expt}(i,j) - c_{p,theor}(i,j)\right\}\right]^2. \quad (20)$$

In Eq. (20), the index i means the experimental scan whereas the index j denotes the points of each scan. Regarding the fitting procedure written here, the strong correlation among the parameters has already been reported. In fact, a correlation that both A and T_2 decreased with the increase in B could be seen for DSC data in this work. Then, the parameter B was kept fixing at first, whereas the others were changed successively in the search routine.

3. Experimental section

3.1. Materials

The monomer, 6-(4′-cyanobiphenyl-4-yloxy) ethyl-acrylate was synthesised following literature procedures by starting from 4-cyano-4′hydroxybiphenyl [45,46] The polymer PCB2A was prepared by radical polymerisation in an absealed ampoule for 30 h at 333 K. A mixture of toluene and dimethyl sulfoxide was used as the polymerisation solvent. PCB2A was purified by repeated precipitation, and fractionated by GPC. The weight-average molecular weight (M_w) of each fractionated polymer was determined by GPC calibrated with polystyrene standards. The molecular weight and the index of distribution, M_w/M_n of fractionated samples are summarised in Table 1, together with T_g, $T_{N\text{-}I}$.

3.2. Methods

JEOL JNM-LA-500, proton NMR and Nicolet Inc. MAGNA FT-IR were used to verify the chemical structure of the monomer synthesised. The elemental analyses were also carried out for the monomer to confirm sample identification; the results were as follows; $C_{18}H_{15}O_3N$(293) Calc.: C73.72; H5.12; N4.78. Found: C76.69; H4.44; N5.52. GL-Sciences gel permeation chromatograph equipped with 504R differential refractometer was used to determine M_w of the fractionated samples; tetrahydrofuran was used as the mobile phase at 1 mL min^{-1} and Shodex gel columns were calibrated with polystyrene standards. The phase behaviour was observed under OLYMPUS AX-70 polarising optical microscope (POM) equipped with Mettler–Toledo FP90 hot stage.

SEIKO DSC200 was used to obtain $c_p(T)$ curve from the DSC curve of dq/dt vs temperature, where the calibration was carried out with reference to c_p of Indium of 200, 250, 298, 400, 500 K [47]. In the measurements, the sample was (i) first maintained at 140 °C, well above T_{cl} for 5 min to erase any previous thermal history; (ii) cooled to a specified ageing temperature, T_A with a cooling rate of 12 °C/min; (iii) annealed for the ageing period t_A; and (iv) cooled to a temperature well below T_g (T_g—50 °C); then the DSC curve was recorded on heating with a rate of 5 °C/min to determine the enthalpy loss, $\Delta H(t_A, T_A)$. Before each measurement, the reference scan was recorded following steps (i), (ii) and (iv), from which $c_p(T)$ was fitted to the linear equation of;

$$c_p(T) = aT + b. \quad (21)$$

In determining the coefficients of the range higher than T_g, the temperature regions of the fittings are always chosen to the lower outside of the tail of $T_{N\text{-}I}$ endothermic peak to avoid the influence of the peak on the linear equation. The coefficients determined are shown in Table 1. The error level of the coefficients is very important because it is sensitive to the calculation of $S_c^{eq}(T)$ of Eq. (13), and consequently to that of $c_p(T)$; the error level is directly reflected by the uncertainties of DSC raw data, which was described in the results shown in Fig. 3.

Table 1
Characteristics of PCB2A sample and coefficients of the linear equation fitted for $c_p(T)$ obtained by the reference scan of $t_A = 0$.

Sample code	M_w	M_w / M_n	T_g / °C	$T_{N\text{-}I}$ / °C	$T<T_g$		$T>T_g$	
					$a\times10^3$	b	$a\times10^3$	b
P2A_1	1.5×10^5	1.25	80	104	–	–	–	–
P2A_2	1.0×10^5	1.70	80	102	–	–	–	–
P2A_3	2.7×10^4	1.26	75	102	6.4	−1.27	6.1	−1.00
P2A_4	1.7×10^4	1.17	75	100	7.5	−1.61	7.4	−1.45

4. Results

4.1. Phase behaviour

As shown in Table 1, both T_g and $T_{N\text{-}I}$ varied with the molecular weight of the polymer. $T_{N\text{-}I}$ was determined with the endothermic peak appeared in the heating DSC scan. T_g was determined with the plot of H vs temperature [48], which is shown below in detail. The variations of the transition temperatures with the molecular weight are approximately consistent with earlier works carried out for the cyanobiphenyl polymer with different spacer length [32,49–51], which were easily grasped. In contrast, the kinetics from isotropic to nematic transitions of PCB2A were complex. The results of cooling DSC scan with a rate of −0.1 °C/min are shown in Fig. 2. It is obvious that the exothermic peaks in the curves of P2A_1 and P2A_2 have disappeared whereas those of other two samples remain. The shoulders on the DSC curves can be seen as an indicator of the glass transition on samples of P2A_3 and P2A_4, whereas there are no shoulder near glass transition region for P2A_1 and P2A_2. From the temperature jump observation in POM, it was found that it took relatively long time for the isotropic-nematic transition of P2A_1 and P2A_2; approximately 60 min that the nematic phase appeared by the temperature jump from 105 to 90 °C. DSC scan speed of −0.1 °C/min is

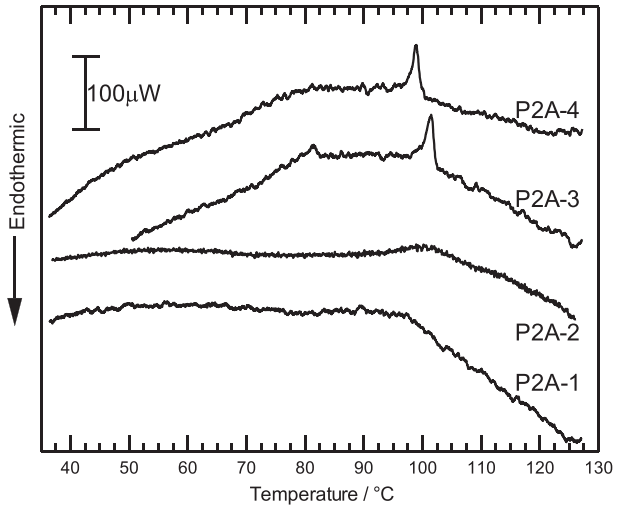

Fig. 2. Cooling DSC curves for PCB2A samples. The cooling rate is −0.1 °C/min.

still too fast to follow the isotropic-nematic transition, and consequently the exothermic peak cannot be observed. The slow dynamics induced by a large molecular weight is shown here as an example of a research object of interest [52,53].

4.2. Enthalpy relaxation

The heating DSC curves for P2A_4 with the ageing of $T_A = 64$ °C was shown in Fig. 3 to illustrate $\Delta H(t_A, T_A)$ which can be evaluated by the area bounded by the DSC curves with and without ageing. As shown in Fig. 3 the temperature of the endothermic peak shifted higher with the ageing time. Because the peak temperature corresponds to the process of enthalpy recovery during the heating of the aged sample, the increase in the peak temperature may be attributed to the decrease of the molecular mobility of the chain segments as a consequence of the decrease in free volume [32].

The uncertainties of DSC curves must be alluded here; they are important because most of the data discussed in this work are directly, or indirectly, derived from DSC curve. In fact, the series of DSC scans were repeated for P2A_3 of $T_A = 58$ °C and P2A_4 of $T_A = 64$ °C, after an interval of a half year. In consequence, the heat flow curves of P2A_4 acquired with that interval were in good agreement with those data shown in Fig. 3 in the temperature ranges of 50–64 °C and 90–96 °C, showing that the baselines before and after the glass transition did not shift. The coefficients of Eq. (21) were determined in the temperature ranges of 57–64 °C and 90–92 °C. As for the area bounded by the DSC curves, which is equivalent to $\Delta H(t_A, T_A)$, the errors found for the experiments of $t_A = 34$–3963 min, P2A_4 of $T_A = 64$ °C were less than 180 mJ/g; the difference of 180 mJ/g corresponds to that of 0.03 in the level of $-\ln\phi$ appeared in Fig. 5. The extent of scattering of $-\ln\phi$ data was estimated and indicated as the error bar in Fig. 5 for plots of $T_A = 58$ °C(P2A_3) and $T_A = 64$ °C(P2A_4). This error level will not prevent the progress of the discussion taking into account the fact that the calculations of AES and TNM framework are carried out on the basis of the derived data of τ, β of Eq. (4) and $\Delta H(t_A, T_A)$, which are closely related with the plot of $-\ln\phi$ and t_A.

By the conversion from DSC raw data of Fig. 3 to $c_p(T)$ data, the plot of H vs temperature was constructed using the relation of enthalpy and the heat capacity as expressed in Eq. (22).

$$H(T_2) = H(T_1) + \int_{T_1}^{T_2} c_p(T)\mathrm{d}T \tag{22}$$

The result was shown in Fig. 4 for the reference scan (i.e. $t_A = 0$) of P2A_4. The extrapolation line was also added to Fig. 4 to illustrate the determination of $\Delta H(\infty, T_A)$ for an arbitrary ageing temperature. As can be seen in Fig. 3, the tail of $T_{N\text{-}I}$ endothermic peak appears at temperatures higher than 92 °C, which will influence the determination of $\Delta H(\infty, T_A)$. It should be noted that the calculation values of $c_p(T)$ obtained with Eq. (21) were used to avoid the influence instead of the experimental values in constructing the H vs temperature plot in the range higher than 92 °C. Using the straight line shown, we can extrapolate the equilibrium values for P2A_4 at temperatures lower than the glass transition, and hence the value of $\Delta H(\infty, T_A)$ is determinable.

For samples of P2A_3 and P2A_4, ϕ values were calculated as a function of t_A from data of $\Delta H(t_A, T_A)$ and $\Delta H(\infty, T_A)$. Whereas, for

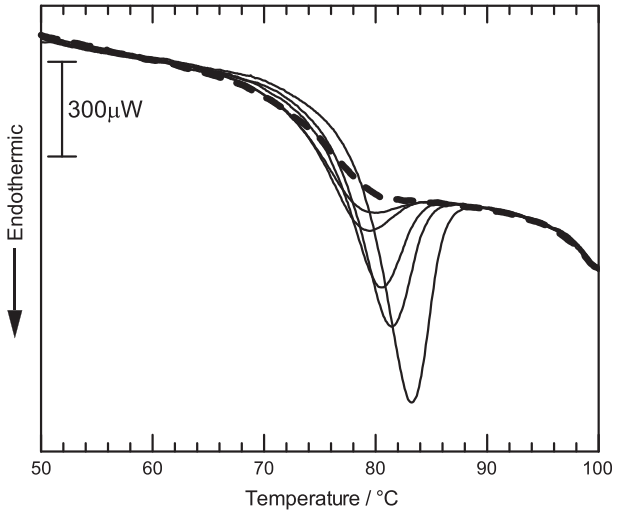

Fig. 3. Heating DSC curves of P2A_4 annealed at $T_A = 64$ °C. Samples were annealed; $t_A = 34$, 64, 305, 725, 3963 min in the order of decreasing intensity. The heating rate is 5 °C/min. The dashed line is the data for reference scan (that is, $t_A = 0$).

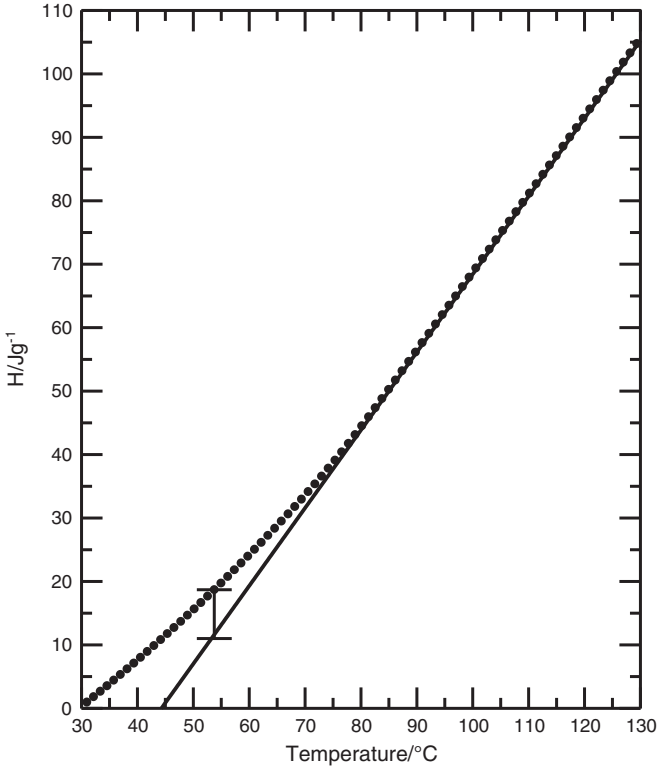

Fig. 4. The relation of enthalpy and temperature obtained with Eq. (22) from $c_p(T)$ of heating scan for P2A_4. $T_1 = 30$ °C was used. The vertical bar at $T_A = 54$ °C is equivalent to $\Delta H(\infty, 54$ °C).

P2A_1 and P2A_2, the calculation of ϕ was stopped since the shoulders of T_g that appeared on heating measurements were not so clear in comparison with other two samples that further analyses based on TNM framework seemed to be difficult. Note that, still P2A_1 and P2A_2 showed enthalpy overshoots like those seen in Fig. 3 upon the thermal ageing experiments.

In Fig. 5 shown is the relation of $-\ln\phi$ and t_A for P2A_3 and P2A_4. From the slope and the intersection, the parameters of β and τ are determined, which can be used for further analyses. As a result, β value increased with the increase in T_A. As is known generally, β is an index of broadness for the distribution of τ in the multiple relaxation processes. Further, the fact that β gets closer to 1 implies the processes approach to the single relaxation of Maxwell type. It can be considered that the relaxation process is averaged with the enhancement of segmental motion owing to the rise in the ageing temperature.

Next, the reduced plot of ϕ vs $(t_A/\langle\tau\rangle)$ was constructed for ϕ functions of P2A_3 to verify the master curve (see Fig. 6), where $\langle\tau\rangle$ is the average relaxation time [54].

$$\langle\tau\rangle = \frac{\tau}{\beta}\Gamma(1/\beta). \tag{23}$$

Fig. 6 was estimated for the plot of $T_A = 58$ °C from the extent of scattering of ϕ data. It was clarified that $\langle\tau\rangle$ is the shift factor in the time domain, in other words, the thermal ageing of t_A and T_A effects on PCB2A with thermo-rheological simplicity [55]. WLF plot of $(T_A - T_g)$ / log $(\langle\tau\rangle)$ vs. $(T_A - T_g)$ with T_g value seen in Table 1 for P2A_3 and P2A_4, was constructed and shown in Fig. 7 to evaluate the constants of C_1 and C_2 on the basis of the following equation.

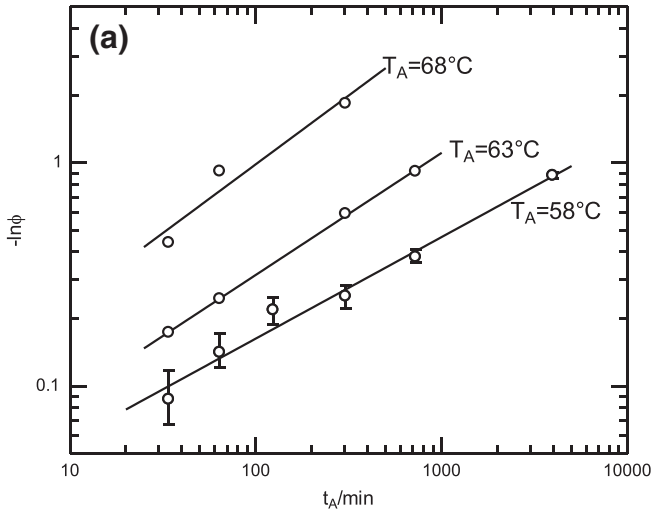

Fig. 5. Double logarithmic plots of $-\ln\phi$ vs t_A for P2A_3 (a) and P2A_4 (b). The ageing temperature, T_A is shown in the figure.

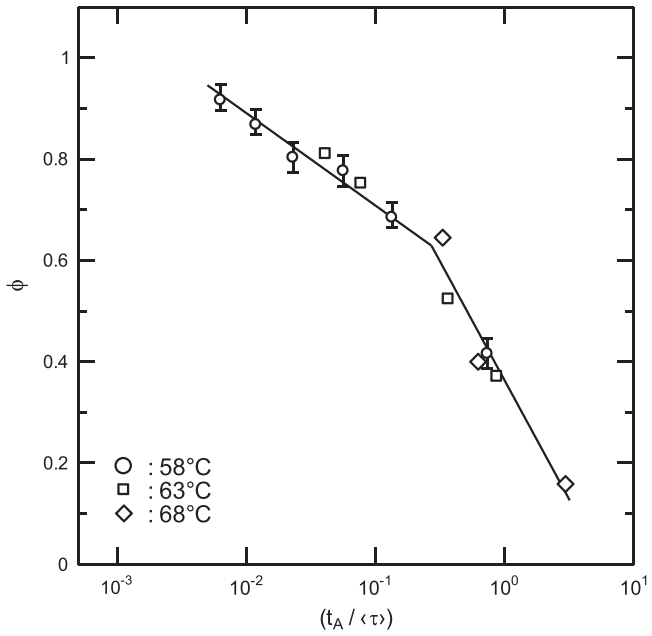

Fig. 6. The reduced plot of the relaxation function obtained for the enthalpy relaxation of P2A_3. The average relaxation time $\langle\tau\rangle$ were calculated with Eq. (23). ϕ values of $T_A = 58$, 63, 68 °C were used as shown in the figure.

$$\log(\langle\tau\rangle) = -\frac{C_1\left(T_A - T_g\right)}{C_2 + \left(T_A - T_g\right)} \tag{24}$$

The plot showed a single linear relation, which implies that any remarkable difference cannot be seen between these two samples for relaxation processes. $C_1 = 14.29$ and $C_2 = 39.9$ were obtained here; they were lower than the values of $C_1 = 17.44$ and $C_2 = 51.6$ known as the universal constants. If the free volume theory can be applied to this result, the volume expansion at T_g is larger than those of many polymers for which the universal constants can be applied; this must be characteristic of the comb-like polymer.

5. Discussion

5.1. Activation energy spectrum

The decrease in enthalpy caused by thermal ageing at constant temperature is related to the approach of PCB2A sample to the equilibrium state, and is controlled by molecular processes being accompanied by the local dynamics; activation energies of the dynamics, E, are distributed over a continuous spectrum. AES of P2A_3 and P2A_4 samples are shown in Fig. 8 where $P(E)$ is expressed as the relative number, that is, the height of the largest peak in the AES becomes equivalent to 100.

The spectra obtained show a peak and tend to zero for small and large energies, which is the well-known behaviour as the first derivative of the stretched exponential function. While the peak height gets lowered for P2A_3 in the order of increasing T_A, its variation for P2A_4 was not monotonous against T_A, which can be accounted for with the factors to influence the peak height. The factors are $\Delta H(\infty, T_A)$, β and T_A; as the increase in $\Delta H(\infty, T_A)$ the peak height increases. β has an influence on both the peak height and the spectrum width. Furthermore, as the rise in T_A, the peak height increases but the effect of T_A is not so

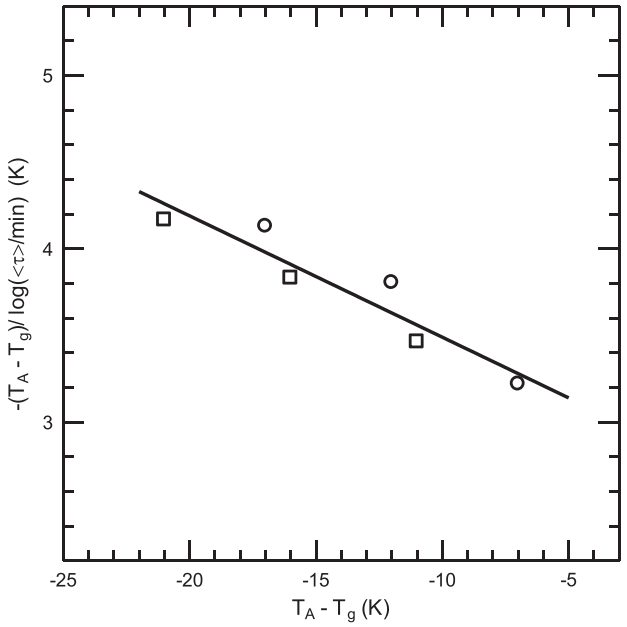

Fig. 7. WLF plot based on T_g shown in Table 1 for P2A_3 (circle) and P2A_4 (square).

strong as that of β, $\Delta H(\infty, T_A)$. These three parameters are in competition with each other to determine the peak height of AES. As a result, the temperature dependence of the peak height for P2A_4 was not simple. The energy where the maximum locates, which is denoted by E_{top}, is in the range from 100 to 120 kJ/mol for both P2A_3 and P2A_4 upon T_A employed in the experiments. The tailings of the peaks shifted in accordance with T_A.

E_{top} shifted to a higher energy as the ageing temperature lowered; the energies required to activate the local dynamics at lower temperature for the progress of the relaxation are higher than those considered at higher temperature. A comparison of E_{top} was tried here with the value found in the literature. Although the reports on activation energies for polymers with cyanobiphenyl group are limited, as an analogue, the viscosity for polymers with cyanophenyl benzoate groups in the side chain can be seen. The activation energy is reported as $E_{visc} = 108$ kJ/mol, which is almost in the same range as observed in this study [56].

Although the relaxation process is somewhat ambiguous with respect to the participant of the local dynamics, the fact that E_{top} locates roughly around 110 kJ/mol can be a characteristic feature of the enthalpy relaxation of PCB2A. In order to make E_{top} value comparable with the energy constant of B shown in the later section, it is assumed here that the molecular weight of the participant is approximately equivalent with that of the repeating unit of PCB2A, denoted by

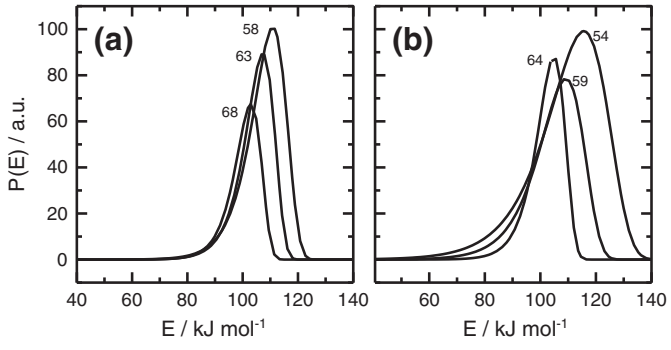

Fig. 8. Activation energy spectra for the enthalpy relaxations of PCB2A, (a) P2A_3, (b) P2A_4. T_A of the ageing experiment is shown in the figure.

M_{unit}; then we obtain 110 kJ/mol = 380 J/g for E_{top} as $M_{unit} = 293.3$. Although we have no grounds for the assumption given here, the repeating unit can be the primal measure for counting the size of the participant. The resulting value of E_{top} appears in the interpretation of SC model parameter shown below. A similar argument can be seen in the paper of Gómetz et al.; it is assumed that the molecular weight of chain segment for the conformational rearrangement can be substituted by that of the monomeric unit, in the discussion of B parameter appeared in SC model [57].

5.2. TNM framework

The magnitude of the enthalpy overshoot in DSC curve observed for the ageing sample increased with the ageing time as shown in Fig. 3. The DSC curve was converted to $c_p(T)$ curve with reference to c_p of indium and then the data fitting of SC model was performed. The fitting procedure resulted in the data output of a single set of parameters ($\ln A$, B, T_2, δ) which minimises the data deviation of Eq. (20). Regarding the fitting procedure demonstrated in this study, some correlation among the parameters has already been reported in the literature. In fact, a correlation that both $\ln A$ and T_2 decreased with the increase in B could be seen for our DSC data. The fixed values of B were chosen as $500 \le B \le 3000$ with an interval of 500 after the manner shown in the literatures [37,57,58]. For the respective B values, different parameter sets are found. Taking the correlation into account, $\ln A$, T_2 and δ were changed successively for given B by the search routine to fit the model $c_p(T)$ curve to the experimental $c_p(T)$ data. The model data were calculated under a constant T_A with the β value determined from $-\ln\phi$ vs t_A plot.

The examination of SC model was performed by a simultaneous fit of six experimental scans at $T_A = 54$ °C for P2A_4. The results of the best fit corresponding to $B = 500$ J/g are shown in Fig. 9 [59]; the set of parameter acquired, ($\ln A$, B, T_2, δ) = (−22, 500, 35, 0.145). The ability of the SC model was acceptable in reproducing the position and shape of $c_p(T)$ peak which is the indication of enthalpy recovery, and the result of the parameter set was also used to construct the plot of τ^{eq} vs T shown below. The results of the best fit corresponding to $B = 500$ J/g for simultaneous fits of five scans at $T_A = 59$ °C and six scans at $T_A = 64$ °C for P2A_4 are shown in Fig. 10; the sets of parameter acquired were indicated in the figure caption.

The examinations were also conducted for DSC scans of P2A_3, which result of simultaneous fit using $B = 500$ J/g on seven scans at $T_A = 58$ °C was shown in Fig. 11; the parameters acquired, ($\ln A$, B, T_2, δ) = (−22, 500, 41, 0.141). As for the result of P2A_3, the ability to reproduce $c_p(T)$ curve was in the same level as the result for P2A_4. Then, the parameter set was forwarded to the next process of constructing the plot of S_c vs T.

From the inspection of $c_p(T)$ curve, some features of the material response after the thermal treatments can be given. The position of the endothermic peak experimentally observed, slightly shifted to higher temperature side by the rise in T_A. Taking the results of Fig. 3 into consideration, the peak position is influenced by both T_A and t_A. Also, it has relationship with the process of recovery of enthalpy, and thus recovery of entropy, during the heating of the aged sample. The position shift is, in general, accounted for by the evolution of the out-of-equilibrium configurational entropy. In order to verify the relationship of the peak position and configurational entropy, the calculated $S_c(t)$ data of $B = 500$ obtained for scans of P2A_3, $T_A = 58$ °C were plotted in Fig. 12; data of $t_A = 64$, 124 were removed to prevent them from overlapping. Fig. 12 contains $S_c^{eq}(T)$ for reference, which was calculated by Eq. (13) with the parameter of T_2 obtained in the search routine performed. Schematic diagram like Fig. 12 is often used to account for the effect of ageing on physical properties. In particular, the diagram of enthalpy–temperature curve can be seen in much of the literature to illustrate enthalpic T_g, unrelaxed enthalpy, equilibrium glassy state and so on. By following the curve of $S_c(t)$

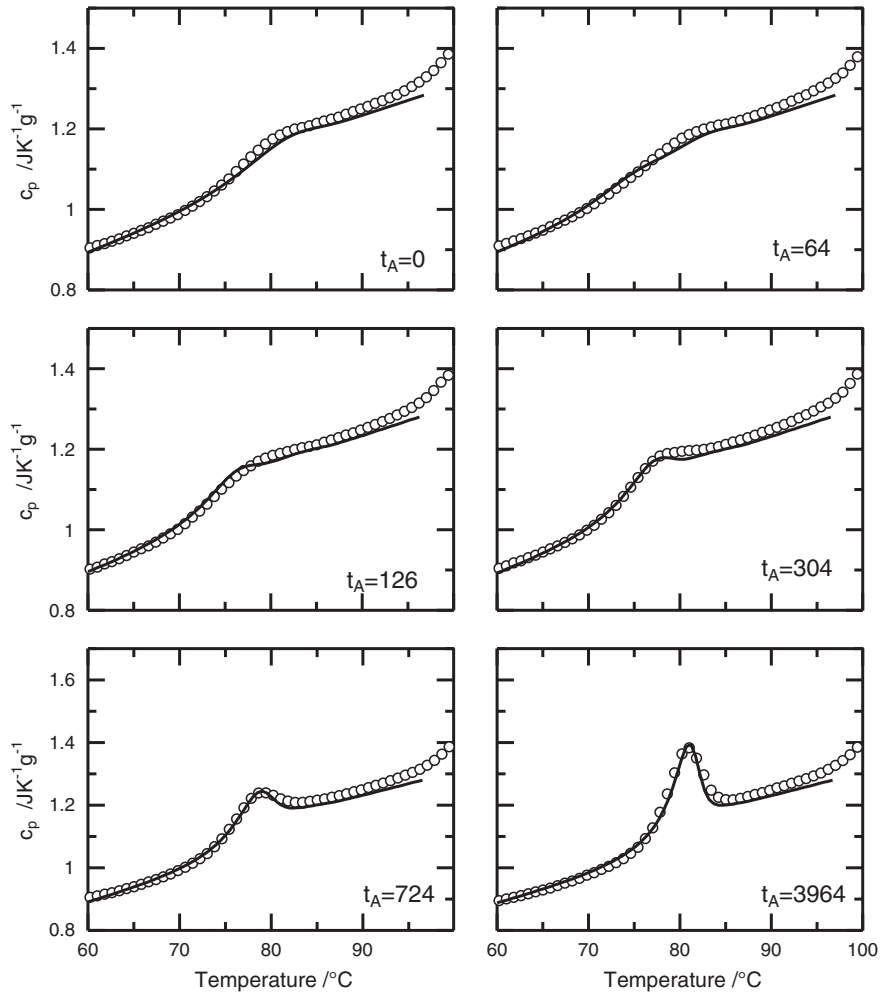

Fig. 9. Simultaneous fit of DSC scans recorded after the ageing of $T_A = 54$ °C for P2A_4. Solid lines and plots are the calculation and experimental data respectively. The set of ($\ln A$, B, T_2, δ) used is (−22, 500, 35, 0.145).

along with the temperature profile shown in the experimental section, it becomes clearer to realise the relation of ageing and the intensity of overshoot. In the cooling process, the sample follows the line of $S_c^{eq}(T)$ from high temperature, then deviates from it to the plot of $t_A = 0$ with further cooling below T_g, finally reaches T_A. At T_A, the sample experiences the ageing by lowering its $S_c(t)$; the amount of the decrease in $S_c(t)$ depends on t_A as shown by the relaxation function of Eq. (4), where the sample reaches $S_c^{eq}(T)$ at equilibrium. After the ageing, the sample follows the plot of the respective ageing time with further cooling as well as the heating scan process.

In the heating scan process, $S_c(t)$ of the aged samples shows plateau value up to $T \approx 70$ °C, then it increases with the rise in temperature. After passing T_g, it continues to increase and finally meets up with the line of $S_c^{eq}(T)$. While $S_c(t)$ of $t_A = 0$ is always higher than $S_c^{eq}(T)$ until the meeting, $S_c(t)$ of respective t_A once gets lower than $S_c^{eq}(T)$, then increases rapidly to meet up with $S_c^{eq}(T)$; the rapid increase corresponds with the recovery of entropy. It is clear that the rapid increase shifts to the higher temperature side as the increase in t_A, which coincides with the shift of the peak position shown in the DSC curve.

The $S_c(t)$ data of $B = 500$ obtained on P2A_4 for three scans of (t_A, T_A) = (724, 54), (724, 59), (725, 64), i.e., those displayed in Figs. 9 and 10, were examined for the relationship between T_A and the temperature range where the entropy recovery takes place in the heating scan. As a result, it was revealed that the temperature range shifted to the higher side with the increase in T_A.(The figure was omitted.) The rise in T_A, in other words, the increase in the relaxation rate, is the reason for the shift of the temperature range of the entropy recovery. Obviously, the faster the relaxation rate is, the larger for same t_A the amount of the decrease in $S_c(t)$ is. If the amount of $S_c(t)$ decrease is larger, the entropy recovery takes place in the higher temperature side like $S_c(t)$ curves in Fig. 12; consequently, the $c_p(T)$ peak appears at higher temperature.

We have to verify whether the different parameter sets found in the search routine would not contradict each other. The equilibrium relaxation time, τ^{eq} characterises that the relaxation mechanism was calculated for P2A_4 with different sets of ($\ln A$, B, T_2) parameters of $T_A = 64$ °C, and plotted against temperature in Fig. 13. Also in the work of Andreozzi et al., the issue of different parameter sets was investigated using the plot of τ^{eq} vs $1/T$. The plots of different parameters were indistinguishable in the narrow temperature range near T_g [31]. Or conversely, the plots of τ^{eq} vs $1/T$ become distinguishable for different sets of parameter if one moves away from T_g. In fact, the further away one moves from T_g, more and more the differences of the plot become significant. Nevertheless, Andreozzi et al. showed the standpoint to support that the different parameters express a single relaxation mechanism. The τ^{eq} vs temperature plots obtained in our study also show that they are in no difference around 75 °C of T_g, and diverge for low and high temperature. We concluded the relaxation mechanisms are different for different parameter sets.

Further investigation was carried out by analysing the strong correlations of B–T_2 and B–$\ln A$. The correlation can be accounted for with

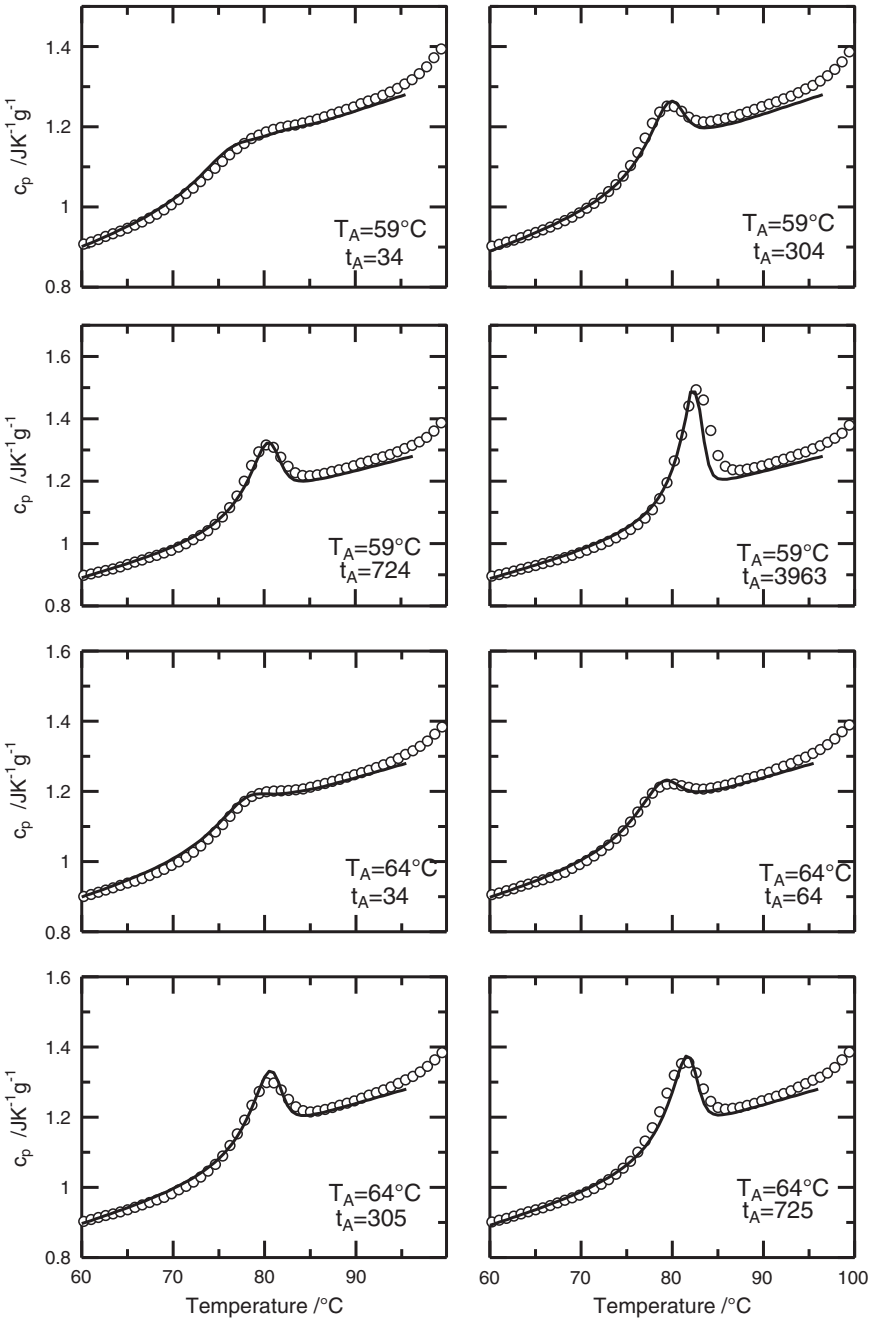

Fig. 10. Simultaneous fit of DSC scans recorded after the ageing of $T_A = 59$ °C and 64 °C for P2A_4. Solid lines and plots are the calculation and experimental data respectively. The sets of ($\ln A$, B, T_2, δ) used are (−23, 500, 36, 0.132) for $T_A = 59$ °C and (−27, 500, 34, 0.154) for $T_A = 64$ °C.

taking the logarithm of Eq. (10). When $\ln A$ was a fixed constant, $S_c(t)$ increases, and hence T_2 decreases with the increase in B so that τ value is kept invariable. When T_2 was kept constant, it means $S_c(t)$ is constant, $\ln A$ decreases with the increase in B to keep τ value invariable.

The correlations observed were shown in Fig. 14. The interesting results seen in Fig. 14 are the dependences of T_2 and $\ln A$ on the ageing temperature for a fixed B. For $B = 3000$, both T_2 and $\ln A$ vary according to the change in T_A, whereas they are nearly unvarying for $B = 500$. When B was fixed to be 500, T_2 and $\ln A$ are uniquely determined irrespective of T_A, which is a preferable result to express the relaxation mechanism by SC model. If it was chosen larger than 500 in fixing B, such a unique determination is no longer realised in the simultaneous fit of both P2A_3 and P2A_4. Furthermore, the scatters of both T_2 and $\ln A$ against T_A become roughly broad as the rise in B. These results suggests that the parameter set obtained for $B = 500$ or smaller is most applicable to $c_p(T)$ curves of ageing temperatures in wide range.

Careful consideration should be given to matters of the correlation of $\ln A$, B and T_2 because the error level in the parameter output strongly influences the plots of B–T_2 and B–$\ln A$ shown in Fig. 14. In getting the parameter output, values of the average square deviation defined by Eq. (20) were in the range of $0.051 < \sigma_a < 0.201$ for P2A_3 and $0.069 < \sigma_a < 0.203$ for P2A_4. In some cases, the fittings were not as tight as those found in the literatures [18,19,41]. In addition, the resource of the computer system can affect the simultaneous fit. In the parameter search of $\ln A$ and T_2, the variables used in the successive substitutions were rounded off at the decimal point. Accordingly,

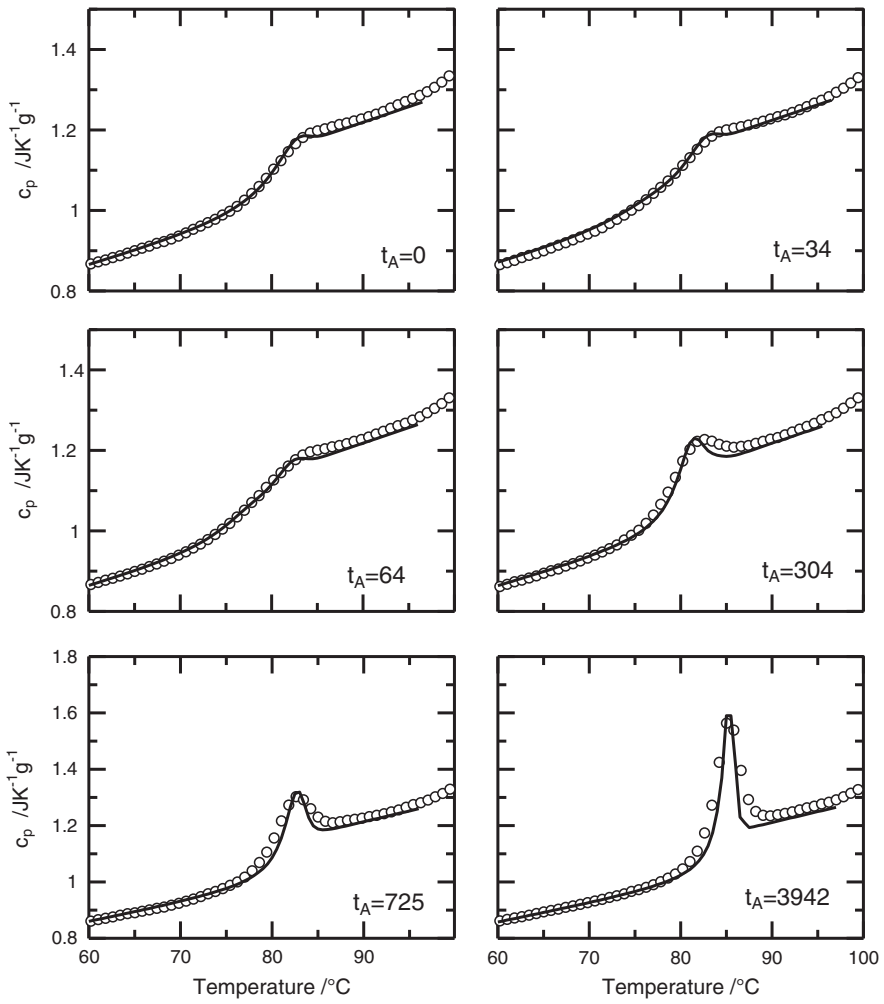

Fig. 11. Simultaneous fit of DSC scans recorded after the ageing of $T_A = 58$ °C for P2A_3. Solid lines and plots are the calculation and experimental data respectively. The set of ($\ln A$, B, T_2, δ) used is (-22, 500, 41, 0.141).

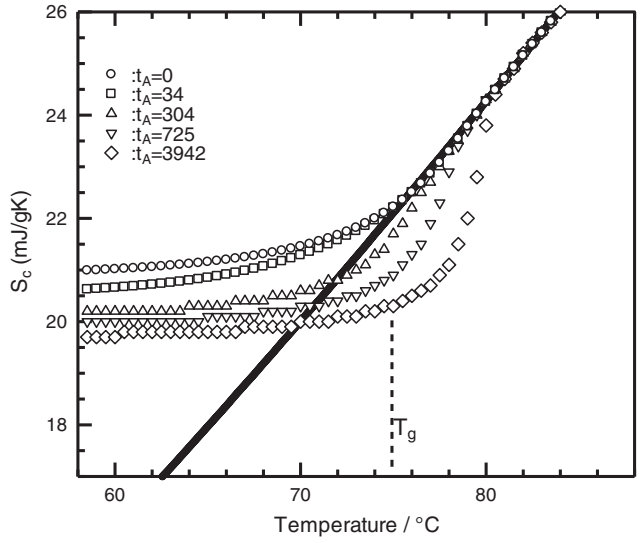

Fig. 12. The relation of $S_c(t)$ and temperature of P2A_3 for different ageing time at $T_A = 58$ °C. $S_c(t)$ were calculated with a set of ($\ln A$, B, T_2) = (-22, 500, 41) for the out-of-equilibrium configurational entropy. The solid line represents $S^{eq}{}_c(T)$.

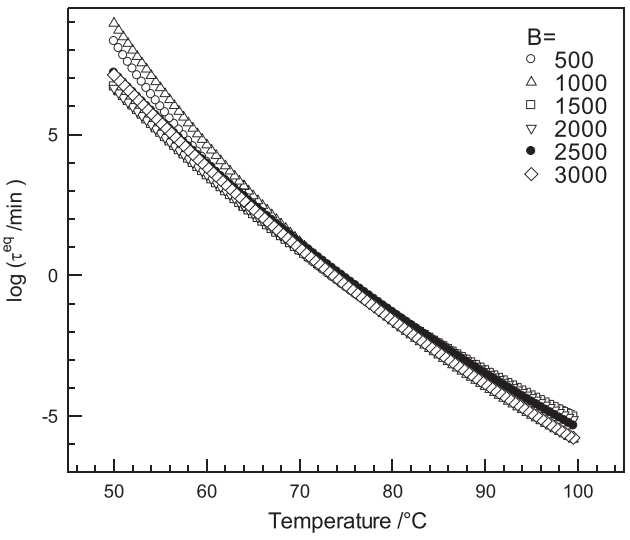

Fig. 13. The plot of $\log(\tau^{eq}/\text{min})$ as a function of temperature for P2A_4. Different sets of ($\ln A$, B, T_2) parameters obtained in the search routine of $T_A = 64$ °C with fixing B values shown in the figure were used to calculate τ^{eq}.

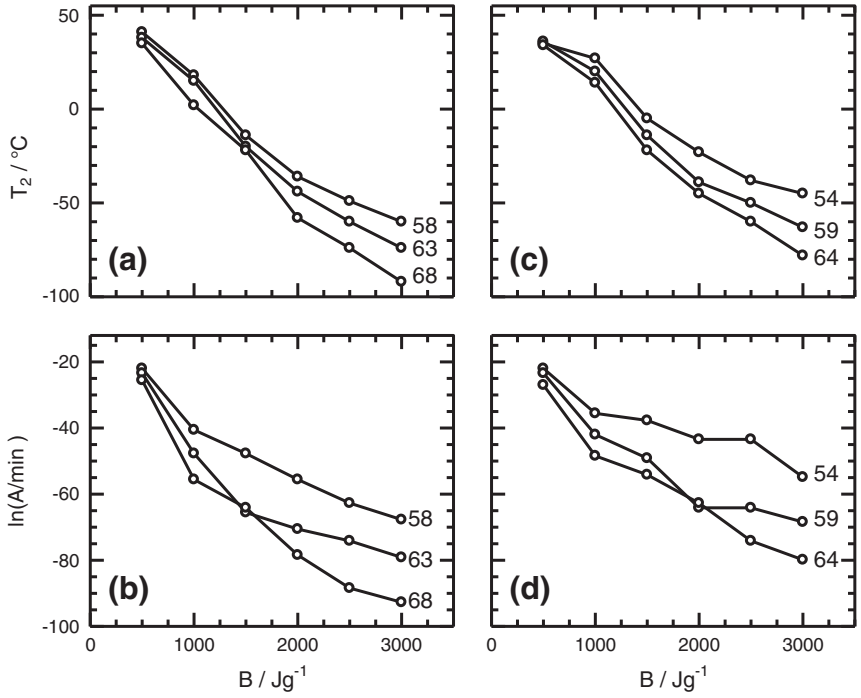

Fig. 14. The relations of T_2 vs B, ln$A$ vs B obtained as an output of the search routine for the simultaneous fit. (a) and (b) are the relations of T_2 vs B, ln$A$ vs B, respectively, for P2A_3. (c) and (d) are the relations for P2A_4. T_A of the ageing experiment is shown in the figure.

the plots shown in Fig. 14 are to include error bars of ± 1. If the iterative routines below the decimal points are allowed, fine adjustment would be made for ln$A$ and T_2.

In connection with the result shown in Fig. 14, the physical meaning of A must be mentioned. As a matter of fact, it is inconceivable that the parameter of ln$A$ takes such a low value as lower than -30. Eq. (2) was derived originally in the Adam–Gibbs theory, where the pre-exponential factor A is the order of the period of atomic vibrations which would remain the only relevant characteristic times in the high temperature limit. If the period of atomic vibrations is estimated as in the order of 10^{-13} s, it would be $\ln(A/\mathrm{min}) \approx -25$ [26,60,61]. All the values of ln$A$ shown in Fig. 14 are not suitable except for the values obtained in the search routine of $B = 500$. If this argument is applied to the results of $c_p(T)$ fittings shown in many literatures, some questions need to be addressed to the data of A which is shorter than the period of atomic vibrations.

Interestingly, the result that B of 500 J/g or smaller is most suitable can be interpreted in connection with the activation energy shown in Fig. 8. The value 380 J/g could be seen for E_{top} with assuming the molecular weight of the participant of local dynamics. It sounds plausible that E_{top} is approximately equivalent with B taking into account that the energies of most relaxation processes are concentrated near E_{top}.

Although the discussion given above implies that B can be substituted by E_{top}, we must be cautious before concluding this by taking the analysing procedures into consideration. The independent determination for B value has not been accomplished when referring to earlier works regarding SC model. In these works, the simultaneous fittings are carried out for $c_p(T)$ curves of different T_A. On the other hand, the fittings shown in our work are performed within a single T_A, moreover, β are determined with other experimental results. It is necessary to consider these analysing processes in detail for the elucidation of the relationship between E_{top} and the energy constant of B.

6. Concluding remarks

The kinetics of the isotropic-nematic transition of PCB2A are influenced by the molecular weight (M_w). Very slow transition to make the exothermic peak in DSC curve disappear was observed for the samples of higher M_w, whereas the DSC peaks appeared as usual in the isotropic–nematic transition for samples of lower M_w. The influence of M_w could not be seen for the behaviour of enthalpy relaxation. Using the enthalpy data obtained from samples of lower M_w, time–temperature reducibility was applied to the relaxation function, where the shift factors showed WLF type temperature dependence. The constants of WLF equation were lower than the universal constants, showing that the volume expansion of PCB2A at T_g is relatively higher; that is, there shows a characteristic feature of comb-like polymer for PCB2A. SC model makes it possible to calculate $c_p(T)$ data in accordance with the thermal ageing carried out at the experiment; it has sufficient prediction power. B of the energy constant within model parameters obtained as the data output of the search routine was discussed in relation to E_{top}, the energy in which AES maximum locates. Although indisputable data to show directly that E_{top} is equivalent with B could not be acquired, the incorporation of AES model helps the analyses of enthalpy relaxation in terms of the energy value related to the segment motion participating in the relaxation process.

References

[1] J.M. Hutchinson, Prog. Polym. Sci. 20 (4) (1995) 703–760.
[2] I.M. Hodge, J. Non-Cryst. Solids 169 (1994) 211–266.
[3] G.B. McKenna, J. Non-Cryst. Solids 172–174 (1994) 756–764.
[4] L.C.E. Struik, Polymer 38 (1997) 4053–4057.
[5] A. Tverjanovich, J. Non-Cryst. Solids 298 (2002) 226–231.
[6] I. Echeverria, P.-C. Su, S.L. Simon, D.J. Plazek, J. Polym. Sci., Part B: Polym. Phys. 33 (1995) 2457–2468.
[7] G.B. McKenna, J. Phys. Condens. Matter 15 (2003) S737–S763.
[8] A. Lee, G.B. McKenna, Polymer 31 (1990) 423–430.
[9] Y. Miyamoto, K. Fukao, Phys. Rev. Lett. 88 (22) (2002) 225504.
[10] L. Grassia, A. D'Amore, J. Rheol. 53 (2009) 339–356.
[11] L. Grassia, A. D'Amore, J. Polym. Sci., Part B: Polym. Phys. 47 (2009) 724–739.
[12] L. Grassia, A. D'Amore, Phys. Rev. E 74 (2006) 021504.
[13] G.W. Scherer, J. Am. Ceram. Soc. 67 (7) (1984) 504–511.
[14] Narayanaswamy, J. Am. Ceram. Soc. 54 (10) (1971) 491–498.
[15] A.Q. Tool, J. Am. Ceram. Soc. 29 (1946) 240–253.
[16] C.T. Moynihan, A.J. Easteal, M.A. DeBolt, J. Tucker, J. Am. Ceram. Soc. 59 (1976) 12–16;
M.A. DeBolt, A.J. Easteal, P.B. Macedo, C.T. Moynihan, ibid 59 (1976) 16–21.
[17] I.M. Hodge, Macromolecules 20 (1987) 2897–2908.

[18] L. Andreozzi, M. Faetti, M. Giordano, D. Palazzuoli, F. Zulli, Macromolecules 36 (2003) 7379–7387.
[19] L. Andreozzi, M. Faetti, F. Zulli, M. Giordano, Macromolecules 37 (2004) 8010–8016.
[20] I.M. Hodge, Macromolecules 19 (1986) 936–938.
[21] J.M.G. Cowie, R. Ferguson, Macromolecules 22 (1989) 2312–2317.
[22] S.L. Simon, Macromolecules 30 (1997) 4056–4063.
[23] J.M. O'Reilly, I.M. Hodge, J. Non-Cryst. Solids 131 (1991) 451–456.
[24] U. Fotheringham, R. Müller, K. Elb, A. Baltes, F. Siebers, E. Weiß, R. Dudek, Thermochim. Acta 461 (2007) 72–81.
[25] S.L. Simon, P. Bernazzani, J. Non-Cryst. Solids 352 (2006) 4763–4768.
[26] P. Richet, J. Non-Cryst. Solids 355 (2009) 628–635.
[27] T. Kanaya, K. Kaji, Adv. Polym. Sci. 154 (2001) 87–141.
[28] T.F. Schatzki, J. Polym. Sci. 57 (1962) 337–356.
[29] B. Valeur, J.P. Jarry, F. Geny, L. Monnerie, J. Polym. Sci. Polym. Phy. Ed. 13 (1975) 667–674;
B. Valeur, L. Monnerie, J.P. Jarry, ibid 13 (1975) 675–682.
[30] R.E. Robertson, J. Polym. Sci. Polym. Symp. 63 (1978) 173–183.
[31] L. Andreozzi, M. Faetti, M. Giordano, D. Palazzuoli, Macromolecules 35 (2002) 9049–9056.
[32] C. Alvarez, N.T. Correia, J.J. Moura Ramos, A.C. Fernandes, Polymer 41 (2000) 2907–2914.
[33] D. Lacey, G. Nestor, M.J. Richardson, Thermochim. Acta 238 (1–2) (1994) 99–111.
[34] V. Lorenzo, J.M. Perena, E. Perez, R. Benavente, A. Bello, J. Mater. Sci. 32 (1997) 3601–3605.
[35] M.R.J. Gibbs, J.E. Evetts, J.A. Leake, J. Mater. Sci. 18 (1983) 278–288.
[36] A. Munoz, F.L. Cumbrera, R. Marquez, Mater. Chem. Phys. 21 (1989) 279–291.
[37] J.L. Gómez Ribelles, M. Monleón Pradas, A. Vidaurre Garayo, F. Romero Colomer, J. Más Estellés, J.M. Meseguer Dueñas, Polymer 38 (1997) 963–969.
[38] G. Adam, J.H. Gibbs, J. Chem. Phys. 43 (1965) 139–146.
[39] J.M. Hutchinson, S. Montserrat, Y. Calventus, P. Cortes, Macromolecules 33 (2000) 5252–5262.
[40] J.L. Gómez Ribelles, M. Monleón Pradas, Macromolecules 28 (1995) 5867–5877.
[41] L. Andreozzi, M. Faetti, F. Zulli, M. Giordano, Eur. Phys. J. B 41 (2004) 383–393.
[42] N.M. Alves, J.L. Gómez Ribelles, J.F. Mano, Polymer 46 (2005) 491–504.
[43] J. Mandel, The statistical analysis of experimental data, Dover Pub. Inc., New York, 1984.
[44] J.A. Nelder, R. Mead, Comput. J. 7 (1965) 308–313.
[45] M.H. Litt, W.-T. Whang, K.-T. Yen, X.-J. Qian, J. Polym. Sci. A. Polym. Chem. 31 (1993) 183–191.
[46] V.P. Shivaev, S.G. Kostromin, N.A. Platé, Eur. Polym. J. 18 (1982) 651–659.
[47] H.K. Cammenga, W. Eysel, E. Gmelin, W. Hemminger, G.W.H. Höhne, S.M. Sarge, Thermochim. Acta 219 (1993) 333–342.
[48] M.J. Richardson, N.G. Savill, Polymer 16 (1975) 753–757.
[49] M.V. Piskunov, S.G. Kostromin, L.B. Stroganov, V.P. Shivaev, N.A. Platé, Macromol. Chem., Rapid Commun. 3 (1982) 443–447.
[50] S.G. Kostromin, R.V. Talroze, V.P. Shivaev, N.A. Platé, Makromol. Chem. Rapid Commun. 3 (1982) 803–808.
[51] T.I. Gubina, S. Kise, S.G. Kostromin, R.V. Talrose, V.P. Shivaev, N.A. Platé, Liq. Cryst. 4 (1989) 197–203.
[52] E.M. Terentjev, Nat. Mater. 1 (2002) 149–150.
[53] L. Cipelletti, L. Ramos, J. Phys. Condens. Matter 17 (2005) R253–R285.
[54] C.P. Lindsey, G.D. Patterson, J. Chem. Phys. 73 (1980) 3348–3357.
[55] J.D. Ferry, J. Am. Chem. Soc. 72 (1950) 3746–3752.
[56] W. Rupp, H.P. Grossmann, B. Stoll, Liq. Cryst. 3 (1988) 583–592.
[57] J.L. Gómez Ribelles, A. Vidaurre Garayo, J.M.G. Cowie, R. Fergusom, S. Harris, I.J. McEwen, Polymer 40 (1998) 183–192.
[58] J.L. Gómez Ribelles, M. Monleón Pradas, A. Vidaurre Garayo, F. Romero Colomer, J. Más Estellés, J.M. Meseguer Dueñas, Macromolecules 28 (1995) 5878–5885.
[59] The $c_p(T)$ curve of $t_A = 64$ min was included in Figure 9, while its ϕ value was not included in Figure 5(b), because the value of $\Delta H(t_A, T_A)$ was nearly equivalent with zero. That is to say, at $T_A = 54$ °C where the relaxation time is the longest in the measurements of this work, $t_A = 64$ min is shorter than the time when $\Delta H(t_A, T_A)$ becomes appreciable. The same behaviour can be seen for the creep compliance of polyetherimide with physical ageings (see ref. 6.).
[60] J.C. Dyre, T. Hechsher, K. Niss, J. Non-Cryst. Solids 355 (2009) 624–627.
[61] C.A. Solunov, J. Non-Cryst. Solids 352 (2006) 4871–48769.